J Electr Eng Technol.2018; 13(1): 430-437
http://doi.org/10.5370/JEET.2018.13.1.430

ISSN(Print) 1975-0102
ISSN(Online) 2093-7423

# Improved Attenuation Estimation of Ultrasonic Signals Using Frequency Compounding Method

**Hyungsuk Kim*, Jaeyoon Shim* and Seo Weon Heo†**

**Abstract** – Ultrasonic attenuation is an important parameter in Quantitative Ultrasound and many algorithms have been proposed to improve estimation accuracy and repeatability for multiple independent estimates. In this work, we propose an improved algorithm for estimating ultrasonic attenuation utilizing the optimal frequency compounding technique based on stochastic noise model. We formulate mathematical compounding equations in the AWGN channel model and solve optimization problems to maximize the signal-to-noise ratio for multiple frequency components. Individual estimates are calculated by the reference phantom method which provides very stable results in uniformly attenuating regions. We also propose the guideline to select frequency ranges of reflected RF signals. Simulation results using numerical phantoms show that the proposed optimal frequency compounding method provides improved accuracy while minimizing estimation bias. The estimation variance is reduced by only 16% for the un-compounding case, whereas it is reduced by 68% for the uniformly compounding case. The frequency range corresponding to the half-power for reflected signals also provides robust and efficient estimation performance.

**Keywords**: Ultrasound, Attenuation, Frequency compounding, Reference phantom method, Quantitative ultrasound

## 1. Introduction

Ultrasonic attenuation in soft tissues caused by signal absorption and scattering aggravates conventional gray-scale B-mode images by either shadowing or enhancement effects for regions of relatively higher or lower attenuation. However, this attenuation is also closely related to the diagnostic information from the medium scanned, and provides a fundamental background for further analysis of other medical ultrasonic parameters that include sound speed, backscatterer size, and spacing in Quantitative Ultrasound (QUS). In consequence, the quantitative estimation of attenuation has been steadily investigated in the literature for decades, and there have been many algorithms published to estimate ultrasonic attenuation from backscattered RF (radiofrequency) signals or envelope data of analytic signals in both the time and frequency domains. Applications of ultrasonic attenuation to differentiate between the normal and benign tissues include liver diseases [1-4], and other areas, such as breast [5-8], bone [9-12], cervical [13-15] and thyroid [16] diseases diagnosis.

In general, the attenuation property of propagated acoustic waves in soft tissues shows frequency-dependent behavior, which means higher frequency components decay faster than lower ones. Hence the reflected RF signals are commonly analyzed in the frequency domain using the Fourier transform to estimate attenuation properties quantitatively [17-22]. Estimation methods in the frequency domain generally provide robust results to additive noises, while those in the time domain are easier to implement. The spectral domain method known as the reference phantom method [20] measures the ratio of power spectra between the reference phantom and the sample, and effectively compensates the diffraction effects of propagating waves. It also easily eliminates system-dependent parameters such as transmit pulse shape and beam focus, and provides very accurate and stable estimation results in the region where no backscatterer property changes occur. However, the critical factor for applying quantitative analysis to real clinical practice is minimizing the estimation variance for multiple independent estimates.

The characteristic of the ultrasonic attenuation in soft tissues has been generally modeled to be linearly frequency-dependent as the wave propagates, and the attenuation property does not vary much depending on the frequency. Therefore the conventional estimation method was to fix some specific frequency (usually center frequency of the modulated ultrasound signal) and estimate the attenuation coefficient at that frequency component. However, it is known that the Gaussian noise or scattering interferences can hurt the accuracy of the attenuation estimation significantly. Those noise and interferences are generally frequency-dependent, so if we combine multiple estimates

† Corresponding Author: School of Electronic and Electrical Engineering, Hongik University, Korea. (seoweon.heo@hongik.ac.kr)
* Department of Electrical Engineering, Kwangwoon University, Korea. ({hskim, jyshim}@kw.ac.kr)
Received: November 26, 2016; Accepted: July 27, 2017

at different frequencies together then the estimation accuracy may be improved.

In this paper, we propose an improved attenuation estimation method by compounding individual attenuation estimates, calculated in several different frequency regions. The classical frequency compounding techniques have been mainly applied to reduce speckles and/or enhance contrast in B-mode images [23,24]. And the centroid downshift method [18], in a broad sense, which calculates the spectral centroid of short-gated RF signal could be considered as one of means for frequency compounding technique, but it does not account for the noise characteristics as well as reflecting the properties of ultrasonic pulses. Since the power spectrum of short RF segment of a transmit pulse is generally modeled as Gaussian distribution in the frequency domain, the signal-to-noise ratio is also different for each frequency component. In addition, acoustic noises might be added while ultrasonic waves penetrating through soft tissues. Therefore simple averaging technique for multiple estimates which are estimated at different frequencies could not improve estimation performances in both accuracy and repeatability.

To effectively compound multiple estimates, we first derive the mathematical formulations for the given problem based on the AWGN channel noise model. While the conventional frequency compounding methods simply apply the uniform averaging for individual estimates, the proposed method provides the framework for compounding multiple estimates under stochastic noise model. We then solve the optimization problem to maximize the signal-to-noise ratio at then given frequency component, and obtain the optimal weights for compounding the multiple estimates of several frequency regions. This optimization framework would be extended with other ultrasonic noise model under a different situation, and could be used to derive appropriate weights for optimal compounding.

We show three ways of frequency compounding methods and investigate the numerical simulation results to compare the estimation performances. We also propose the guideline for selecting frequency ranges to improve estimation performance by the experimental results using numerical tissue-mimicking phantoms.

This paper is organized as follows: Section II presents a brief summary of the reference phantom method and the mathematical formulations of the problem based on the stochastic channel model. In Section III, we solve the optimization problem to derive the optimal weighting coefficients for compounding in the frequency region, and also propose three possible compounding methods. Section IV shows simulation results using numerical tissue-mimicking phantoms to compare the estimation performances of accuracy and variances. We also compare estimation performances with respect to the range of frequency components (or the number of frequency components) for the compounding technique. The following section summarizes the contributions of this paper and shows the application areas.

## 2. Theoretical Background

### 2.1 The reference phantom method

Assuming the Born approximation, the intensity of reflected RF signal in the frequency domain, $I(f,z)$, can be represented by the product of the transmit pulse $G(f)$, the diffraction property $D(f,z)$, and the attenuation and backscatterer terms of $A(f,z)$ and $B(f)$ as:

$$I(f,z) = G(f) \cdot D(f,z) \cdot A(f,z) \cdot B(f) \tag{1}$$

where $z$ denotes the depth from the transducer. In (1), the first two terms, $G(f)$ and $D(f,z)$, are considered system-dependent properties, while the terms of $A(f,z)$ and $B(f)$ are directly related to the scanned tissue properties. In the reference phantom method, the system-dependent terms are effectively eliminated by dividing the intensity of backscattered signals from a sample by that from a reference phantom whose attenuation properties are already known [20]. The ratio of backscattered signals, $RI(f,z)$, between the sample and reference phantom is represented by the ratio of the only tissue-dependent terms, given by:

$$RI(f,z) = \frac{I_s(f,z)}{I_r(f,z)} = \frac{G(f)D(f,z)A_s(f,z)B_s(f)}{G(f)D(f,z)A_r(f,z)B_r(f)} = \frac{A_s(f,z)B_s(f)}{A_r(f,z)B_r(f)} \tag{2}$$

where the subscripts $s$ and $r$ represent the sample and reference, respectively. Since the attenuation property in soft tissues is generally assumed to be linearly frequency-dependent [21], the ratio of backscattered signals shown in (2) can be represented by:

$$RI(f,z) = \frac{B_s(f)}{B_r(f)} \exp\{-4(\beta_s - \beta_r)fz\} \tag{3}$$

where $\beta$ is termed the attenuation coefficient in units of dB/cm/MHz. After taking the natural logarithm of the above equation, we apply least square line fitting with respect to the propagation depth $z$ to the log of the intensity ratio, $L(f,z)$, and finally obtain the attenuation difference as follows:

$$\beta_\Delta(f) = \beta_r - \beta_s = \frac{1}{4f}\frac{dL(f,z)}{dz} \tag{4}$$

Note that we assume the attenuation property in soft tissues is linearly proportional to the frequency, so theoretically the above equation can be calculated at any single frequency component.

### 2.2 Noise modeling

For the case where a random noise is added to the backscattered signals, the ratio of power spectra between the sample and reference phantom in the frequency domain in (2) is rewritten and given by:

$$\begin{aligned} RI(f,z) &= \frac{I_s(f,z)}{I_r(f,z)} \\ &= \frac{G(f)D(f,z)A_s(f,z)B_s(f)+N_s(f)}{G(f)D(f,z)A_r(f,z)B_r(f)+N_r(f)} \\ &= \frac{B_s(f)A_s(f,z)\left\{1+\frac{N_s(f)}{G(f)D(f,z)A_s(f,z)B_s(f)}\right\}}{B_r(f)A_r(f,z)\left\{1+\frac{N_r(f)}{G(f)D(f,z)A_r(f,z)B_r(f)}\right\}} \end{aligned} \tag{5}$$

where $N_r(f)$ and $N_s(f)$ represent noise random processes of the reference and sample, respectively. To obtain the final attenuation difference, we can derive the natural logarithm of this ratio as follows:

$$\begin{aligned} L(f,z) = \log RI(f,z) &= \log\frac{B_s(f)}{B_r(f)} + 4(\beta_r-\beta_s)fz \\ &+ \log\left(\frac{1+\frac{N_s(f)}{G(f)D(f,z)A_s(f,z)B_s(f)}}{1+\frac{N_r(f)}{G(f)D(f,z)A_r(f,z)B_r(f)}}\right) \end{aligned} \tag{6}$$

Assuming that the intensity of noise is generally much smaller than that of the backscattered RF signals both for the reference and sample (i.e., $(f) \ll G(f)D(f,z)$ $A(f,z)B(f)$), and using the Taylor series approximation of $\log(1+x) \approx x$ if $|x| \ll 1$, then the third term of the above equation is approximated by:

$$\begin{aligned} &\log\left(\frac{1+\frac{N_s(f)}{G(f)D(f,z)A_s(f,z)B_s(f)}}{1+\frac{N_r(f)}{G(f)D(f,z)A_r(f,z)B_r(f)}}\right) \\ &\approx \log\left(1+\frac{N_s(f)}{G(f)D(f,z)A_s(f,z)B_s(f)}\right) \\ &\approx \frac{N_s(f)}{G(f)D(f,z)A_s(f,z)B_s(f)} \\ &= \frac{N_s(f)}{G(f)D(f,z)\exp(-4\beta_s fz)\,B_s(f)} \end{aligned} \tag{7}$$

which is the inverse of the signal-to-noise ratio of the backscattered RF signal. Using this approximation result, the noise term in the nonlinear function in (6) can be simplified as the additive channel noise model given by:

$$L(f,z) = \log\frac{B_s(f)}{B_r(f)} + 4(\beta_r-\beta_s)fz + \frac{N_s(f)}{G(f)D(f,z)\exp(-4\beta_s fz)B_s(f)} \tag{8}$$

To calculate the difference of attenuation coefficients between the sample and reference phantom, we apply (4) to (8), then the results can be represented by:

$$\begin{aligned} \hat{\beta}_\Delta(f) &= \beta_\Delta(f) + \frac{\beta_s N_s(f)}{G(f)D(f,z)\exp(-4\beta_s fz)\,B_s(f)} \\ &= \beta_\Delta(f) + W_s(f) \end{aligned} \tag{9}$$

As shown in (9), the additive noise random process, $W_s(f)$ corrupts the natural logarithm of the power ratio between the sample and reference. If we assume that $\mathrm{E}(N_s(f)) = N_0$ where $N_0$ is the power spectral density of AWGN random process, we can think of $W_s(f)$ as a noise random process that is inversely proportional to the backscattered signal intensity or the signal to noise ratio of the received signal at the frequency $f$.

Therefore, if we obtain attenuation estimates from several different frequency components, we can improve the estimation accuracy and/or reduce the estimation variance by the optimal-weighted compounding the individual estimation results under the stochastic noise model. In the next section, we propose three frequency compounding methods for the reference phantom method, and compare their estimation performances.

## 3. Frequency Compounding Methods

### 3.1 Largest SNR selection (LSS)

The original reference phantom method estimates attenuation coefficients with respect to several single frequency components, and analyzes the frequency-dependency of the attenuation property in soft tissues. The first method of frequency domain compounding is the selection of just one frequency component. This is not a compounding technique, but provides the bottom line of estimation performance for comparison. When we select the frequency at which the attenuation coefficient is calculated, the modulation center frequency of a transmit pulse is one of the candidates where the signal strength might usually be maximum, though sometimes (or in some depths) it might not be correct. The spectral centroid using the power spectrum of the ROI will be an alternative choice of this method, because of the frequency-dependent attenuation property in soft tissues. Otherwise we can choose the best frequency component given by the following optimization process:

$$\begin{aligned} &\tilde{\beta}_\Delta = \hat{\beta}_\Delta(f_k) \text{ where} \\ &f_k = \arg\max_f G(f)D(f,z)\exp(-4\beta_s fz)B_s(f) \end{aligned} \tag{10}$$

where $\hat{\beta}_\Delta(f_k)$ is given by (9).

### 3.2 Uniform Weight Compounding (UWC)

In this compounding method, we average attenuation estimates of each frequency component with equal weights, so the estimation is given by:

$$\tilde{\beta}_\Delta = \frac{1}{N+1}\sum_{k=1}^{N+1}\hat{\beta}_\Delta(f_k) \text{ where } f_k \in \left\{f_c - mf_\Delta : m = -\frac{N}{2} \sim \frac{N}{2}\right\} \quad (11)$$

where $f_c$ may be either the center frequency of a transmit pulse or the centroid of power spectrum at a given depth, and $f_\Delta$ represents the frequency step between adjacent frequency components.

When applying this method, it is critical to choose the appropriate set of frequency components – frequency range and number of components. Adding frequency components from the lower SNR range will degrade the estimation accuracy and variance, especially at deeper depths. The rule of thumb in estimation theory is that the SNR corresponding to the frequencies to be combined should be high enough - for example, larger than 10. In this paper, we compare the estimation performances with respect to the number of frequency components those are averaged, and provide a guideline to select the proper number of frequency components.

### 3.3 Optimal Weight Compounding (OWC)

In this method, we derive the optimal compounding weights for each frequency component to get the maximum SNR at the output of the combiner as follows:

$$\tilde{\beta}_\Delta = \sum_{k=1}^{N}\omega_k\hat{\beta}_\Delta(f_k) \text{ where } \sum_{k=1}^{N}\omega_k = 1, \quad (12)$$

where $\omega_k$ is the compounding weights for the frequency at $f_k$.

To derive the optimal compounding weights, we assume that the estimated attenuation coefficient corresponding to each frequency component is unbiased and not frequency-selective, i.e., $\beta_\Delta(f_k) = \beta_\Delta$. Then the signal-to-noise ratio after the frequency compounding is given by:

$$SNR = \max_{\{\omega_k:\sum_{k=1}^{N}\omega_k=1\}} \frac{\left(\sum_{k=1}^{N}\omega_k\,\beta_\Delta(f_k)\right)^2}{E\left[\left(\sum_{k=1}^{N}\omega_k\,W_S(f_k)\right)^2\right]} = \max_{\{\omega_k:\sum_{k=1}^{N}\omega_k=1\}} \frac{(\beta_\Delta)^2}{E[(\sum_{k=1}^{N}\omega_k\,W_S(f_k))^2]} \quad (13)$$

If we assume that the noise signal $W_S(f_k)$ 's are independent and identically distributed of noise random process and the expectation value is $E[|W_S(f_k)|^2] = P_k$, then we can formulate the problem to derive the optimal weight by:

$$\omega_{opt} = \underset{\{\omega_k:\sum_{k=1}^{N}\omega_k=1\}}{\text{argmax}} \frac{(\beta_\Delta)^2}{\sum_{k=1}^{N}{\omega_k}^2 P_k} = \underset{\{\omega_k:\sum_{k=1}^{N}\omega_k=1\}}{\text{argmin}} \sum_{k=1}^{N}{\omega_k}^2 P_k \quad (14)$$

The constrained optimization problem of (14) can be easily solved by the Lagrange multiplier method by transforming (14) into an unconstrained optimization problem as follows:

$$\omega_{opt} = \underset{\{\omega_k,\lambda\}}{\text{argmin}} \sum_{k=1}^{N}{\omega_k}^2 P_k + \lambda\left(\sum_{k=1}^{N}\omega_k - 1\right) \quad (15)$$

By differentiating (15) with respect to $\lambda$ and ${\omega_k}'s$, we obtain:

$2\omega_k P_k + \lambda = 0$ for $k = 1, \cdots, N$ and $\sum_{k=1}^{N}\omega_k = 1$ .

These can easily be shown to be:

$$\omega_{k,opt} = \frac{\frac{1}{P_k}}{\sum_{k=1}^{N}\frac{1}{P_k}} \quad (16)$$

Since $\frac{1}{P_k}$ represents the signal-to-noise ratio of the received signal at the frequency $f_k$, (16) shows that the optimal compounding weights of the frequency component is proportional to the SNR ratio, or to the signal strength of the backscattered signal at the frequency component of $f_k$. This result is similar to the maximal ratio combining method in the wireless communication system.

## 4. Results

In this paper, we use simulated numerical phantoms, which is a frequency-domain model based on the classical diffraction theory for continuous wave propagation [25]. The size of a phantom is 40 mm (width) x 80 mm (height), and it consists of randomly distributed 25 μm glass beads with a sound speed of 1540 m/s. We set the attenuation coefficients of phantoms to 0.3 dB/cm/MHz and 0.5 dB/cm/MHz for the reference phantom and sample, respectively. The entire phantom is divided into small blocks of 4 mm x 4 mm to calculate the block power spectrum, and a block overlap ratio of 50 % is applied in both the axial and lateral directions. The beam focus is set to 40 mm, and each RF segment is tapered by the Hanning window to minimize artifacts of spectral leakage. Table 1

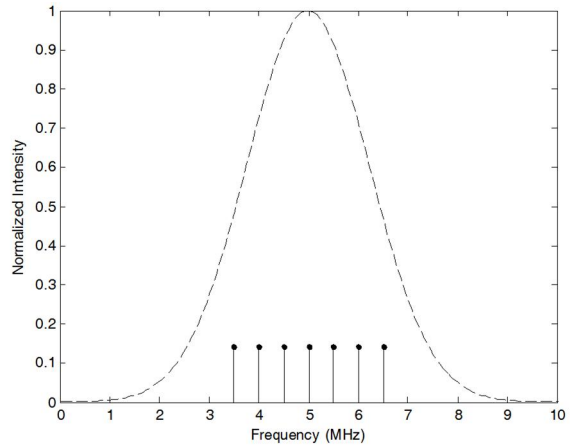


(a)

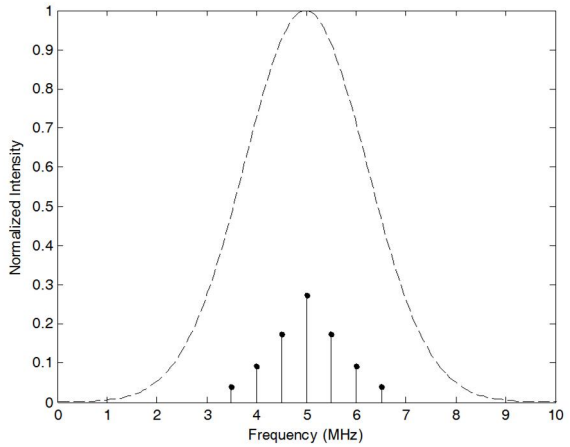


(b)

**Fig. 1.** Illustrative weighting factors of the combining methods. Seven frequency components are selected centered at 5MHz, with a frequency step of 0.5 MHz. The dashed line is assumed to be a power spectrum of the received signals: (a) Uniform weight combining, and (b) Optimal weight combining

shows all of the other simulation parameters.

Fig. 1 shows illustrative weighting factors of the two compounding methods (i.e., UWC and OWC). The power spectrum of received signals is assumed as the Gaussian distribution and its magnitude is normalized by the maximum value. The number of compounding frequency components is set to seven, and the power spectrum of reflected RF signals shown in dashed line is Gaussian, with center frequency of 5MHz. The uniform weight compounding (UWC) method averages seven attenuation estimates between 3.5MHz and 6.5MHz (the frequency step is 0.5MHz) with equal weighting factor of 0.143, while the optimal weight compounding (OWC) averages them with different weighting factors that are proportional to the signal strength, under the assumption of the additive white Gaussian noise model.

**Table 1.** Simulation parameters of a numerical phantom

| | |
|---|---|
| Transducer Type | Linear Array |
| Element Size | 0.2 mm x 10 mm |
| Number of Elements | 128 |
| Element Spacing | 0.2 mm |
| F-number | 2 |
| Center Frequency | 5 MHz |
| Bandwidth | 80 % |
| Beam Focus | 40 mm |

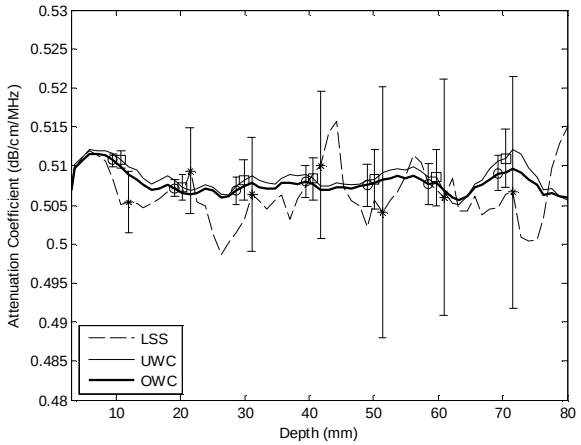


**Fig. 2.** Estimated attenuation coefficients over the entire depth. The attenuation coefficients for the reference phantom and sample are 0.3 and 0.5 dB/cm/MHz, respectively, and the beam focus is set to 40 mm. The errorbars represent the estimation variances at each depth

Fig. 2 shows the estimation results of the attenuation coefficients along the depth. The errorbars represent the estimation variances at each depth. For the LSS method, the centroid of the power spectrum is selected as the compounding frequency component since its SNR is maximized at each depth. For the UWC and OWC methods, frequency components are chosen from the range of 50% FWHM of the power spectrum with a frequency step of 0.1MHz. While the LSS method shows the worst estimation performance with the relatively largest estimation variances, the UWC and OWC methods exhibit similar estimation performances for the entire depth. For the estimation variance, however, the OWC method provides more stable results than the UWC method, especially for the deeper depth that lies after the beam focus. The average estimation variance for the OWC method is only 16% of that for the LSS method, and 68% for the UWC method over the entire depth. Although the difference of attenuation coefficients between the reference phantom and sample generally provides the estimation bias (which is shown by overestimation or underestimation), the OWC method also improves the estimation accuracy for the entire depth.

When the frequency compounding methods are applied, the range of frequency components (or the number of

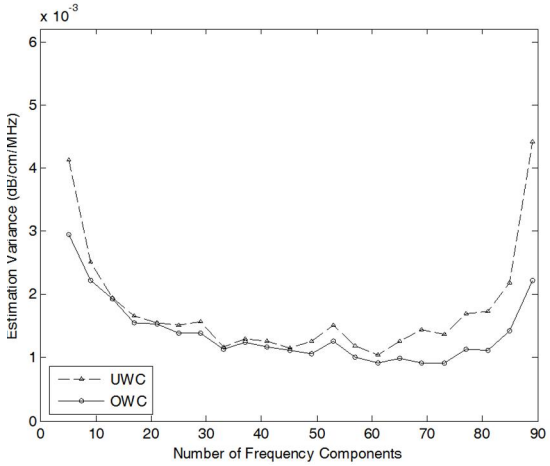


(a)

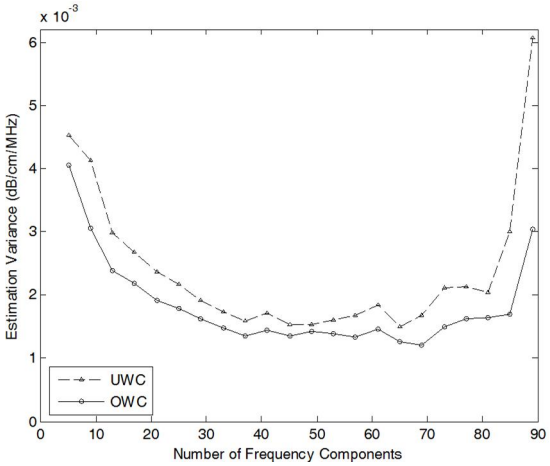


(b)

**Fig. 3.** Estimation variances for the number of frequency components. The frequency components are selected centered at the centroid of power spectrum at each depth with a frequency step of 0.1MHz: (a) 20mm, and (b) 40mm

frequency components) is also related to the estimation accuracy and variance. Since the power intensity of the reflected RF signals rapidly decreases far from the center frequency, the frequency compounding with the proper number (or range) of frequency components may increases computational efficiency while maintaining estimation accuracy. Fig. 3 shows the estimation variances with respect to the number of frequency components for compounding at the two depths of 20mm and 40mm. The simulation parameters are same as the Table 1. In our simulation, we choose the frequency step between adjacent frequencies to be 0.1 MHz, so for example, 40 frequency components means a frequency range between 3 MHz and 7 MHz with a centroid of 5 MHz, which is theoretically the half power range for a transmit pulse of 80% FWHM. Though more frequency components provide smaller initial estimation variances, this no longer applies when too many components are accounted since the signal power may be lower than the noise level. It is difficult to state the optimal number of frequency components for compounding, but in our simulation, the half-power frequency range of the reflected RF signals provides a good rule-of-thumb for a robust and efficient estimation performance.

## 5. Discussion

The proposed method in this paper improves estimation accuracy using the optimal frequency compounding based on the stochastic channel noise model, and we provide additional considerations to compounding individual estimates at different frequencies. We derived mathematical formulation of this compounding problem and optimal compounding methods based on the assumption of the Gaussian noise model.

As for the numerical simulations done in this paper, the lateral dimension of a numerical phantom is not considered for the beam width of an individual A-line. This comes from the limitation of simulation package used, but the authors believe that it does not affect the simulation results shown in this paper because the number of scatterers and distance between beam lines are specified. Since each block that computes power spectrum of echo signals, contains enough number of independent beam lines, its spectral property might be calculated accurately to estimate attenuation coefficients.

The bandwidth of a transmit pulse could be one of parameters to determine the range of frequency components for compounding. It is easily assumed that the lager the usable frequency range, the better the quantitative estimates. In this paper, we proposed an experimental guideline to determine the effective frequency range arguing that whose signal strengths are above half-power. The analytical derivations for the optimal frequency range with respect to the bandwidth of a pulse remain for the further study.

## 6. Conclusion

Quantitative analysis in medical ultrasound has provided much information about the pathological state of soft tissues. The attenuation property of scanned tissues is one of fundamental measures for medical ultrasound, and many researches have striven to improve their estimation accuracy. However, the repeatability of attenuation estimation, which is commonly measured by an estimation variance, is another crucial factor to apply the results of quantitative analysis to clinical practice.

In this paper, we propose a novel optimal compounding method that uses a stochastic noisy channel model for the reference phantom method. This provides very good estimation performances in the uniformly attenuating region, without changes of the backscatterer property. Since the transmit pulse has a maximum energy around

the center frequency, and is generally modeled by a Gaussian distribution, the power intensity of reflected RF signals also exhibits different signal strength at individual frequency components. Therefore, the overall estimation performances might be improved by compounding estimates at multiple frequency components with appropriate weighting factors. Under the assumption of an AWGN channel model, we derive optimal weights for the compounding that are inversely proportional to the noise level, or proportional to the signal strength of the individual frequency component.

Simulation results using numerical phantoms show that estimation results after applying frequency compounding are much better than the single frequency component. For the frequency compounding methods, the proposed OWC method exhibits more accurate and unbiased estimation results than the UWC method, that uniformly averages all frequency components. In our simulation, the frequency range corresponding to the half-power of the reflected RF signal provides a robust and efficient estimation performance.

## Acknowledgement

This work is supported partly by National Research Foundation of Korea(NRF) under Grants NRF-2016 R1D1A1B03930910 and Korea Institute for Advancement of Technology(KIAT) grant funded by the Korean government (MOTIE No. N0001883). It is also conducted during the sabbatical year of Kwangwoon University in 2015.

## References

[1] B. J. Oosterveld, J. M. Thijssen, P. C. Hartman, R. L. Romijn, and G. J. Rosenbusch, "Ultrasound attenuation and texture analysis of diffuse liver disease: Methods and preliminary results," *Phys. Med. Biol*., vol. 36, no. 8, pp. 1039-1064, Aug, 1991.

[2] Y. Fujii, N. Taniguchi, K. Itoh, K. Shigeta, Y. Wang, J. W. Tsao, K. Kumasaki, and T. Itoh, "A new method for attenuation coefficient measurement in the liver: comparison with the spectral shift central frequency method," *Journal of Ultrasound Med*., vol. 21, no. 7, pp. 783-788, Jul, 2002.

[3] M. Meziri, W. C. A. Pereira, A. Abdelwahab, C. Degott, and P. Laugier, "In vitro chronic hepatic disease haracterization with a multiparametric ultrasonic approach," *Ultrasonics*, vol. 43, pp. 305-313, 2005.

[4] R. Bouzitoune, M. Meziri, C. B. Machado, F. Padilla, and W. C. A. Pereira, "Can early hepatic fibrosis stages be discriminated by combining ultrasonic parameters?," *Ultrasonics*, vol. 68, pp. 120-126, 2016.

[5] R. M. Golub, R. E. Parsons, B. Sigel, E. J. Feleppa, J. Justin, H. A. Zaren, M. Rorke, J. Sokil-Melgar, and H. Kimitsuki, "Differentiation of breast tumors by ultrasonic tissue characterization," *Journal Ultrasound Med*., vol. 12, no. 10, pp. 601-608, Oct, 1993.

[6] L. M. Cannon, A. J. Fagan, and J. E. Browne, "Novel Tissue Mimicking Materials for High Frequency Breast Ultrasound Phantoms," *Ultrasound in Med. and Biol*., vol. 37, no. 1, pp.122-135, 2011.

[7] K. Nam, J. A. Zagzebski, and T. J. Hall, "Quantitative Assessment of In Vivo Breast Masses Using Ultrasound Attenuation and Backscatter," *Ultrasonic Imaging*, col. 35, no. 2, pp. 146-161, Apr, 2013.

[8] I. Katz-Hanani, T. Rothstein, D. Gaitini, Z. Gallimidi, and H. Azhari, "Age-Related Ultrasonic Properties of Breast Tissue *In Vivo*," *Ultrasound in Med. and Biol*., vol. 40, no. 9, pp. 2265-2271, 2014.

[9] K. A. Wear, "Characterization of trabecular bone using the backscattered spectral centroid shift," *IEEE Trans. Ultrasonics, Ferroelectrics and Frequency Control*, vol. 50, pp. 402-207, Apr, 2003.

[10] Y. Nagatani, K. Mizuno, T. Saeki, M. Matsukawa, T. Sakaguchi, and H. Hosoi, "Numerical and experimental study on the wave attenuation in bone-FDTD simulation of ultrasound propagation in cancellous bone," *Ultrasonics*, vol. 48, no. 6, pp. 607-612, Nov, 2007.

[11] K. Lee, "Dependences of the Attenuation and the Backscatter Coefficients on the Frequency and the Porosity in Bovine Trabecular Bone: Application of the Binary Mixture Model," *Journal of the Korean Physical Society,* vol. 60, no. 3, pp. 371-775, Feb, 2012.

[12] C. Morin and C. Hellmich, "A multiscale poro-micromechanical approach to wave propagation and attenuation in bone," *Ultrasonics*, vol. 54, pp. 1251-1269, 2014.

[13] Y. Labyed, T. A. Bigelow, and B. L. McFarlin, "Estimate of the attenuation coefficient using a clinical array transducer for the detection of cervical ripening in human pregnancy," *Ultrasonics*, vol. 51, pp.34-39, 2011.

[14] M. Z. Kiss, T. Varghese, and M. A. Kliewer, "Ex vivo ultrasound attenuation coefficient for human cervical and uterine tissue from 5 to 10 MHz," *Ultrasonics*, vol. 51, pp.467-471, 2011.

[15] B. L. McFarlin, V. Kumar, T. A. Bigelow, D. G. Simpson, R. C. White-Traut, J. S. Abramowicz, and W. D. O'Brien Jr., "Beyond Cervical Length: A Pilot Study of Ultrasonic Attenuation for Early Detection of Preterm Birth Risk," *Ultrasound in Med. and Biol*., vol. 41, no. 11, pp.3023-3029, 2015.

[16] J. Rouyer, T. Cueva, T. Yamamoto, A. Portal, and R. Lavarello, "In vivo estimation of attenuation and backscatter coefficients from human thyroids," *IEEE Trans. Ultrasonics, Ferroelectrics and Frequency Control*, vol. 63, no. 9, pp. 1253-1261, 2016.

[17] P. Welch, "The use of fast Fourier transform for the

estimation of power spectra: A method based on time averaging over short, modified periodograms," *IEEE Trans. Audio and Electroacoustics*, vol. 15, no. 2, pp. 70-73, Jun, 1967.

[18] M. Fink, F. Hottier, and J. F. Cardoso, "Ultrasonic signal processing for in vivo attenuation measurement: short time Fourier analysis," *Ultrasonic Imaging*, vol. 5, no. 2, pp. 117-135, Apr, 1983.

[19] T. Baldeweck, P. Laugier, A. Herment, and G. Berger, "Application of autoregressive spectral analysis for ultrasound attenuation estimation: interest in highly attenuating medium," *IEEE Trans. Ultrasonics, Ferroelectrics and Frequency Control*, vol. 42, no. 1, pp. 99-109, Jan, 1995.

[20] L. X. Yao, J. A. Zagzebski, and E. L. Madsen, "Backscatter coefficient measurements using a reference phantom to extract depth-dependent instru-mentation factors," *Ultrasonic Imaging*, vol. 12, no. 1, pp. 58-70, Jan, 1990.

[21] H. Kim and T. Varghese, "Hybrid Spectral Domain Method for Attenuation Slope Estimation," *Ultrasound Medicine and Biology*, vol. 34, no. 11, pp. 1808-1819, Nov, 2008.

[22] K. Samini and T. Varghese, "Optimum Diffraction-Corrected Frequency Shift Estimator of the Ultrasonic Attenuation Coefficient," *IEEE Trans. Ultrasonics, Ferroelectrics and Frequency Control*, vol. 63, no. 5, pp. 691-702, May, 2016.

[23] G. Traney, J. Allison, S. Smith, and O. von Ramm, "A quantitative approach to speckle reduction via frequency compounding," *Ultrasonic Imaging*, vol. 8, no. 3, pp. 151-164, 1986.

[24] J. Sanchez, and M. Oelze, "An ultrasonic imaging speckle-suppression and contrast-enhancement technique by means of frequency compounding and coded excitation," *IEEE Trans. Ultrasonics, Ferroelectrics and Frequency Control*, vol. 56, no. 7, pp. 1327-1339, 2009.

[25] Y. Li and J. A. Zagzebski, "A frequency domain model for generating B-mode images with array transducers," *IEEE Trans. Ultrasonics, Ferroelectrics and Frequency Control*, vol. 46, no. 3, pp. 690-699, May, 1999.

**Hyungsuk Kim** He received a B.S. degree in electrical engineering from Korea Advanced Institute of Science and Technology, Daejeon, Korea, in 1991 and a M.S. degree in electrical and computer engineering from Seoul National University, Seoul, Korea, in 1993. From 1993 to 1999, he worked for Korea Telecom Research Group, Seoul, Korea, working on the design and analysis of data communication networks. He received a Ph.D. degree in electrical and computer engineering from University of Wisconsin - Madison, Madison, WI, in 2008. Since 2008, he has been an associate professor in the department of electrical engineering at Kwangwoon University, Seoul, Korea. His current research interests are in signal and image processing applications for medical ultrasound.

**Jaeyoon Shim** He received a B.S. degree in Computer Science and Engineering from Seoul National University of Technology, Seoul, Korea, in 2010, and a M.S. and a Ph.D. degree in electrical engineering from Kwangwoon University, Seoul, Korea, in 2012 and 2017, respectively. Since 2017, he has been researching as a postdoctoral researcher at Kwangwoon University, Seoul, Korea. His current research interests are in signal and image processing applications for medical ultrasound.

**Seo Weon Heo** He received B.S. and M.S. degrees in electronic engineering from Seoul National University, Korea, in 1990 and 1992, respectively, and a Ph.D. degree in electrical engineering from Purdue University, West Lafayette, IN, in 2001. From 1992 to1998, he was with the Digital Media Research Laboratory, LG Electronics Co. Ltd., Korea. From 2001 to 2006, he worked at the Telecommunication R&D Center, Samsung Electronics Co. Ltd., Korea. Since 2006, he has been a professor with the School of Electronic & Electrical Engineering, Hongik University, Seoul, Korea. His current research interests are in the area of wireless communication, channel coding, and embedded system HW/SW design.